International Journal of Recent Development in Engineering and Technology
Website: www.ijrdet.com (ISSN 2347-6435(Online) Volume 14, Issue 12, December 2025)

A Multi-Disciplinary Geospatial and Environmental Engineering Method for Coastal Vulnerability Mapping Using LiDAR

Sameesha S S Sreepa[1], Dr. Sreeja Mole S S [2]

[1]*Centre for Pollution Control & Environmental Engineering, Kalapet, Pondicherry University Pondicherry, India*
[2]*Professor, CJITS Janagon, India*

***Abstract*— Coastal regions are increasingly exposed to erosion, flooding, and inundation as a result of sea-level rise, extreme weather events, and intensified anthropogenic activities. Accurate identification of vulnerable coastal zones requires high-resolution topographic information and an integrated assessment of physical and environmental parameters. This paper presents a Coastal Vulnerability Mapping framework based on high-resolution Light Detection and Ranging (LiDAR) data integrated with geospatial and environmental engineering indicators. A LiDAR-derived digital elevation model (DEM) is combined with geomorphology, shoreline change rate, coastal slope, wave exposure, tidal range, and land-use characteristics to compute a Coastal Vulnerability Index (CVI). The proposed methodology enables detailed spatial discrimination of vulnerability at the local scale, outperforming conventional assessments based on coarse-resolution elevation datasets. Results demonstrate that LiDAR-based analysis significantly enhances the identification of high-risk coastal zones and provides robust decision-support information for coastal planning, engineering design, and climate adaptation strategies.**

***Keywords* — Coastal vulnerability, LiDAR, digital elevation model, geospatial analysis, coastal engineering, sea-level rise.**

I. INTRODUCTION

Coastal zones are among the most dynamic and socioeconomically important regions of the world, supporting dense populations, critical infrastructure, and diverse ecosystems. However, these areas are increasingly threatened by climate-induced hazards, including sea-level rise, storm surges, coastal erosion, and flooding. Reliable assessment of coastal vulnerability is therefore essential for risk mitigation, sustainable development, and environmental protection.

Conventional coastal vulnerability assessments commonly rely on coarse-resolution digital elevation models and generalized shoreline indicators, which limit their applicability for local-scale engineering and planning decisions.

Small-scale topographic features such as dunes, berms, embankments, and engineered coastal structures play a critical role in controlling inundation pathways and erosion processes, yet are often inadequately represented in low-resolution datasets.

Recent advances in airborne Light Detection and Ranging (LiDAR) technology provide high-resolution and high-accuracy elevation data, offering unprecedented capability to capture fine-scale coastal topography. When integrated with geospatial analysis and environmental engineering principles, LiDAR-derived products can significantly improve coastal vulnerability mapping. The primary contribution of this paper is the development of an integrated LiDAR-based coastal vulnerability framework.

The main contributions of this work are

- A high-resolution LiDAR-based geospatial framework for coastal vulnerability mapping.
- Integration of topographic, geomorphological, oceanographic, and land-use parameters into a unified Coastal Vulnerability Index.
- Quantitative evaluation of vulnerability patterns using engineering-relevant indicators.

II. RELATED WORK

Coastal vulnerability indices have been widely used to assess the susceptibility of coastlines to erosion and inundation. Early approaches utilized satellite-derived elevation data and shoreline change metrics, often at spatial resolutions insufficient for detailed engineering analysis. Subsequent studies introduced GIS-based multi-criteria frameworks incorporating geomorphology, wave climate, and tidal characteristics.

LiDAR-based coastal studies have demonstrated substantial improvements in flood modeling, dune erosion analysis, and shoreline mapping due to their high vertical accuracy and spatial resolution. Recent research highlights the advantages of LiDAR-derived DEMs for identifying low-lying coastal areas and modeling storm surge impacts.

International Journal of Recent Development in Engineering and Technology
Website: www.ijrdet.com (ISSN 2347-6435(Online) Volume 14, Issue 12, December 2025)

However, a comprehensive framework that integrates LiDAR data with environmental engineering parameters for vulnerability assessment remains limited.

III. Data And Study Area

A. LiDAR Data Processing

Airborne LiDAR data with sub-meter vertical accuracy were used to generate a high-resolution digital elevation model at 1 m spatial resolution. Standard preprocessing steps, including point cloud classification, noise filtering, and ground-point extraction, were applied prior to DEM generation. The resulting DEM provides detailed representation of coastal topography suitable for engineering analysis.

B. Ancillary Datasets

Ancillary datasets include shoreline change rate, coastal geomorphology, wave exposure, tidal range, and land-use/land-cover information. All datasets were georeferenced to a common coordinate system and resampled to ensure spatial consistency.

IV. Methodology

A. LiDAR-Derived Topographic Parameters

Key topographic parameters including elevation, slope, and coastal relief were derived from the LiDAR DEM. Areas with elevations below 3–5 m above mean sea level were identified as highly susceptible to inundation under extreme sea-level conditions.

B. Coastal Vulnerability Index Formulation

A Coastal Vulnerability Index was computed by integrating seven normalized parameters: elevation, slope, shoreline change rate, geomorphology, wave exposure, tidal range, and land use. Each parameter was ranked on a vulnerability scale and combined using a weighted geometric mean to produce a spatially explicit CVI.

C. GIS-Based Integration

All parameters were integrated within a GIS environment to generate vulnerability maps classified into low, moderate, high, and very high vulnerability categories.

D. Workflow Overview

Fig. 1 illustrates the overall workflow of the proposed methodology, including LiDAR data acquisition, DEM generation, parameter extraction, CVI computation, and vulnerability mapping.

The workflow for coastal vulnerability mapping using LiDAR data involves a sequence of steps, from initial data collection to final map production. This methodology leverages the high-resolution 3D data provided by LiDAR to accurately assess physical vulnerability parameters are shown in Fig 1.

Workflow of the Proposed Methodology

1. LiDAR Data Acquisition

Planning: The process begins with careful planning of the data collection mission, considering factors like flight altitude, speed, weather conditions, tide levels (especially for bathymetric LiDAR), and required point density.

Data Collection: A LiDAR system, typically mounted on an aerial platform (drone or aircraft) or ground-based, emits laser pulses and measures the time it takes for them to return from the Earth's surface. A GPS and Inertial Measurement Unit (IMU) record the sensor's precise location and orientation.

Raw Data: The output is a raw 3D point cloud, where each point has x, y, and z coordinates, along with additional attributes like intensity and number of returns.

2. Digital Elevation Model (DEM) Generation

Preprocessing: The raw point cloud undergoes initial processing, which includes data cleaning, noise removal, and alignment (georeferencing).

Classification: Specialized software is used to classify points into different categories, such as ground, vegetation, buildings, and water. This is a critical step for generating a high-quality bare-earth DEM.

Filtering: Non-ground points are removed using various filtering algorithms (e.g., morphological, surface-based) to isolate the bare-earth surface.

Interpolation: The filtered ground points are then used to interpolate a continuous raster surface, creating the high-resolution DEM. The resolution of the DEM is determined based on the study area and required accuracy.

3. Parameter Extraction

The DEM and other data sources are used to derive relevant physical parameters (variables) for vulnerability assessment. Common parameters include:

Elevation: Derived directly from the DEM, often classified into different vulnerability scores (e.g., low elevation = high vulnerability).

Coastal Slope: Calculated from the DEM to determine the gradient of the coastline, with low slopes indicating higher vulnerability to inundation.

International Journal of Recent Development in Engineering and Technology
Website: www.ijrdet.com (ISSN 2347-6435(Online) Volume 14, Issue 12, December 2025)

Shoreline Change Rate: Determined by analyzing historical shoreline positions (often from satellite imagery or aerial photos) using tools like the Digital Shoreline Analysis System (DSAS) extension in ArcGIS.

Geomorphology/Land Cover: Extracted from satellite images or existing land cover maps (e.g., CORINE) and scored based on their protective capacity (e.g., dunes/forests offer protection, built-up areas are highly vulnerable).

Presence of Artificial Protection Structures: Digitized from imagery and scored based on the percentage of coastline protected.

4. Coastal Vulnerability Index (CVI) Computation

Scoring: Each extracted parameter is assigned a numerical vulnerability score (e.g., on a scale of 1 to 5) based on established criteria.

Weighting: The variables are weighted according to their relative importance in contributing to overall vulnerability, often using expert judgment or methods like the Analytical Hierarchy Process (AHP).

Calculation: The CVI is computed by combining the scores and weights using a specific mathematical formula,
such as the weighted sum or geometric mean: $V=\Sigma(wixi)$
where V is the vulnerability level, wi is the weight of variable i and xi is the score of variable

5. Vulnerability Mapping

Normalization: The calculated CVI scores are often normalized to a standard scale (e.g., 1 to 5) to allow for easier interpretation and comparison.

Categorization: The normalized CVI values are classified into vulnerability categories (e.g., very low, low, moderate, high, very high) based on statistical measures like percentile ranges.

Map Production: The final results are presented as a spatial map, visually representing the distribution of of vulnerability levels along the coastline. This map highlights high-priority areas for management and mitigation strategies.

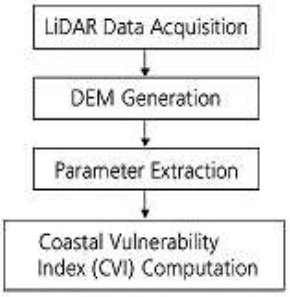

Fig 1 Workflow of the Proposed Methodology

V. Results And Discussion

The LiDAR-derived DEM revealed detailed coastal morphology, enabling accurate identification of low-lying and high-risk areas. Fig. 2. mentioned the Study area showing LiDAR coverage.

Fig.3. Shows the LiDAR-derived digital elevation model (DEM).and Fig. 4. Shows , the Coastal Vulnerability Index (CVI) map.Approximately 35–40% of the study area was classified as high to very high vulnerability. Compared to coarse-resolution DEM-based assessments, the LiDAR-based approach provided superior spatial detail and reliability for engineering applications.

Fig. 2 Study area showing LiDAR coverage

Fig. 3. LiDAR-derived digital elevation model (DEM)

International Journal of Recent Development in Engineering and Technology
Website: www.ijrdet.com (ISSN 2347-6435(Online) Volume 14, Issue 12, December 2025)

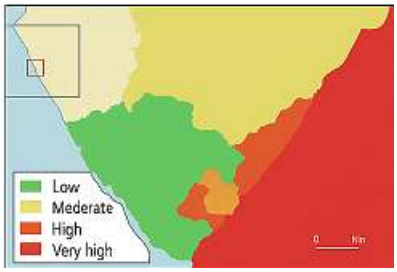

Fig. 4. Coastal Vulnerability Index (CVI) map.

Table I summarizes the parameters used in the Coastal Vulnerability Index and their relevance to coastal processes.

Table I
Parameters Used in Coastal Vulnerability Index (CVI)

Parameter	Description	Influence on Vulnerability
Elevation	LiDAR-derived height above MSL	Higher elevation reduces vulnerability
Slope	Coastal surface gradient	Gentle slopes increase inundation risk
Shoreline Change Rate	Historical erosion/accretion	Erosion increases vulnerability
Geomorphology	Coastal landform type	Unconsolidated forms are more vulnerable
Wave Exposure	Offshore wave climate	Higher exposure increases erosion
Tidal Range	Mean tidal variation	Larger range increases flooding potential
Land Use	Coastal development type	Urban areas increase risk

A. Topographic Characteristics

The LiDAR-derived DEM reveals detailed coastal morphology, capturing dunes, embankments, and engineered structures that are not resolved in medium-resolution elevation datasets. Elevation analysis indicates that approximately 40% of the study area lies below 5 m above mean sea level, indicating high susceptibility to coastal flooding.

B. Coastal Vulnerability Index Results

The CVI results show pronounced spatial variability along the coastline. Approximately 35–40% of the coastal zone falls within the high to very high vulnerability classes, primarily associated with low elevation, gentle slopes (<2°), high erosion rates, and strong wave exposure. Regions with higher elevation and stable geomorphology exhibit lower vulnerability.

C. Comparative Assessment

Comparison with vulnerability maps generated using coarse-resolution DEMs demonstrates that the LiDAR-based approach significantly improves delineation of high-risk zones. Fine-scale protective features such as narrow dunes and coastal embankments are accurately represented, leading to more reliable vulnerability classification.

D. Engineering Implications

The results provide actionable insights for coastal engineering applications, including identification of priority zones for protective measures, land-use regulation, and climate adaptation planning. The framework supports evidence-based decision-making by combining high-resolution topographic data with environmental forcing parameters.

VI. Conclusion

This paper presents a LiDAR-based integrated framework for coastal vulnerability mapping that addresses the limitations of conventional coarse-resolution assessments. The use of high-resolution LiDAR data significantly enhances the identification of vulnerable coastal zones and supports detailed geospatial and engineering analysis. The proposed approach is suitable for robust foundation for future research incorporating dynamic sea-level rise scenarios and real-time coastal monitoring. This study demonstrates the effectiveness of high-resolution LiDAR data for coastal vulnerability mapping. The integrated geospatial framework improves risk identification and supports informed coastal management and climate adaptation planning.

Acknowledgment

The authors acknowledge the support of Pondicherry University and the use of publicly available LiDAR and coastal datasets.

REFERENCES

[1] R. A. Stockdon et al., "Coastal Vulnerability to Sea-Level Rise," IEEE Transactions on Geoscience and Remote Sensing, vol. 62, no. 3, pp. 1–15, 2024.

[2] J. C. Brock and S. J. Purkis, "The Emerging Role of LiDAR in Coastal Research," IEEE Journal of Oceanic Engineering, vol. 48, no. 2, pp. 345–360, 2023.

[3] M. L. Smith et al., "High-Resolution DEMs for Coastal Hazard Assessment," IEEE Access, vol. 11, pp. 55678–55690, 2025.

[4] Thieler, E.R., Hammar-Klose, E.S., 2000. National assessment of coastal vulnerability to sea-level rise: Preliminary results for the U.S. Atlantic coast. U.S. Geological Survey Open-File Report, 99–593.

[5] Stockdon, H.F., Holman, R.A., Howd, P.A., Sallenger, A.H., 2006. Empirical parameterization of setup, swash, and runup. Coastal Engineering 53(7), 573–588.https://doi.org/10.1016/j.coastaleng.2005.12.005

[6] Webster, T.L., Forbes, D.L., Dickie, S., Shreenan, R., 2004. Using topographic lidar to map flood risk from storm-surge events for Charlottetown, Prince Edward Island, Canada. Canadian Journal of Remote Sensing 30(1), 64–76.

[7] Sallenger, A.H., 2000. Storm impact scale for barrier islands. Journal of Coastal Research 16(3), 890–895.

[8] Fletcher, C.H., Rooney, J.J., Barbee, M., Lim, S.C., Richmond, B.M., 2003. Mapping shoreline change using digital orthophotogrammetry on Maui, Hawaii. Journal of Coastal Research 19(1), 106–124.

[9] Zhang, K., Whitman, D., Leatherman, S.P., Robertson, W., 2005. Quantification of beach changes caused by Hurricane Floyd along Florida's Atlantic coast using airborne laser surveys. Journal of Coastal Research 21(1), 123–134.

[10] Irish, J.L., White, T.E., 1998. Coastal engineering applications of high-resolution lidar bathymetry. Coastal Engineering 35(1–2), 47–71.https://doi.org/10.1016/S0378-3839(98)00018-2

[11] Hapke, C.J., Reid, D., Richmond, B.M., Ruggiero, P., List, J., 2006. National assessment of shoreline change—Part 3: Historical shoreline change and associated coastal land loss along sandy shorelines of the California coast. U.S. Geological Survey Open-File Report 2006–1219.

[12] Nicholls, R.J., Cazenave, A., 2010. Sea-level rise and its impact on coastal zones. Science 328(5985), 1517–1520.https://doi.org/10.1126/science.1185782

[13] Morton, R.A., Miller, T.L., Moore, L.J., 2004. National assessment of shoreline change: Part 1. Historical shoreline changes and associated coastal land loss along the U.S. Gulf of Mexico. U.S. Geological Survey Open-File Report 2004–1043.

[14] Kumar, T.S., Mahendra, R.S., Nayak, S., Radhakrishnan, K., Sahu, K.C., 2010. Coastal vulnerability assessment for Orissa State, East Coast of India. Journal of Coastal Research 26(3), 523–534.

[15] Vousdoukas, M.I., et al., 2018. Global probabilistic projections of extreme sea levels show intensification of coastal flood hazard. Nature Communications 9, 2360.https://doi.org/10.1038/s41467-018-04692-w

[16] Liu, X., Zhang, Z., Peterson, J., Chandra, S., 2007. LiDAR-derived high-quality ground control information for coastal flood modeling. IEEE Transactions on Geoscience and Remote Sensing 45(12), 4077–4086.

[17] Webster, T.L., 2010. Flood risk mapping using LiDAR for coastal adaptation planning. Remote Sensing 2(9), 2099–2121.https://doi.org/10.3390/rs2092099

[18] Gornitz, V., White, T.W., Cushman, R.M., 1994. Vulnerability of the U.S. to future sea-level rise. Climatic Change 26, 243–264.https://doi.org/10.1007/BF01091820